ICAS-98-3,8,1

TRAILING-EDGE FLOWS ON HIGHLY-SWEPT WINGS

Andrew Shires*

Defence Evaluation and Research Agency, Bedford, U.K.

Abstract

An experimental and theoretical study is described of the flow over a constant-chord wing with a significant amount of rear camber, for three trailing-edge sweeps 30°, 40° and 50°. The research is aimed at understanding the nature of complex three-dimensional flows and means of controlling these flows for highly swept wings, necessary for low observable combat aircraft. This paper describes the results from a series of wind-tunnel tests in the 13ft x 9ft low speed wind tunnel at DERA Bedford. Oil flow visualisation and analysis of wing pressure and force coefficients has helped to provide a good understanding of the nature of these flows for a range of tunnel speeds and angles of incidence. Calculations have been made with two computational fluid dynamics (CFD) codes, one a Viscous coupled Full-Potential code (VFP) and the other, the SAUNA system, based on a solution of the Reynolds averaged Navier-Stokes equations. The former provides pressure distributions in good agreement with measurement, except for flows with regions of separation. The SAUNA system, using a k-ω two-equation turbulence model, has been used to predict the occurrence of complex three-dimensional separated regions.

Nomenclature

c	wing chord
C_f	skin friction coefficient
C_p	pressure coefficient
M	Mach number
R	Reynolds number, based on wing chord
s	wing semi-span
V	wind tunnel speed
x, y, z	wing ordinates
α	angle of incidence
Δ	incremental part of
Λ	wing leading-edge sweep
∞	conditions far upstream

*Email: ashires@dera.gov.uk

Introduction

Future offensive and reconnaissance combat aircraft will need low observability to enhance current levels of survivability. This necessitates wings with highly swept leading and trailing edges. The magnitude of the wing sweep required differs significantly from that currently used and raises the possibility of three-dimensional separation on the upper surface at moderate angles of incidence. The likelihood of such separation increases if trailing-edge flaps are deployed or, more generally, if wing camber is increased. These separations result in a significant increase in drag and they degrade the buffet characteristics of the aircraft, thus reducing payload fraction/range and/or aircraft agility. Therefore, such configurations represent a high risk from the aerodynamic standpoint. Furthermore, because these flows are complex, prone to boundary layer separation and susceptible to scale or Reynolds number effects, the full-scale or flight characteristics of such configurations cannot be predicted, at present, with confidence either by CFD or from conventional wind-tunnel tests.

The aim of this experimental/theoretical study is to investigate the aerodynamic characteristics at low speeds, of a wing with highly swept leading and trailing edges and also;

(a) to characterise the nature of the flow around the wing for sweeps greater than 30°,
(b) to attempt to control upper surface flow separation using vane-type vortex generators,
(c) to evaluate the capability of current CFD methods for predicting the flowfield around the wing.

Two series of tests in the 13ft x 9ft low speed wind tunnel at DERA Bedford provided force and pressure measurements and flow visualisation photographs for wing sweeps of 30°, 40° and 50°.

After describing the experiment, the flows over the basic wing and methods of controlling them, the paper continues by describing results of predictions by two CFD methods of differing complexities, from a viscous coupled full-potential method to one based on a solution of the Reynolds averaged Navier-Stokes equations.

21st ICAS Congress
13-18 September 1998
Melbourne, Australia

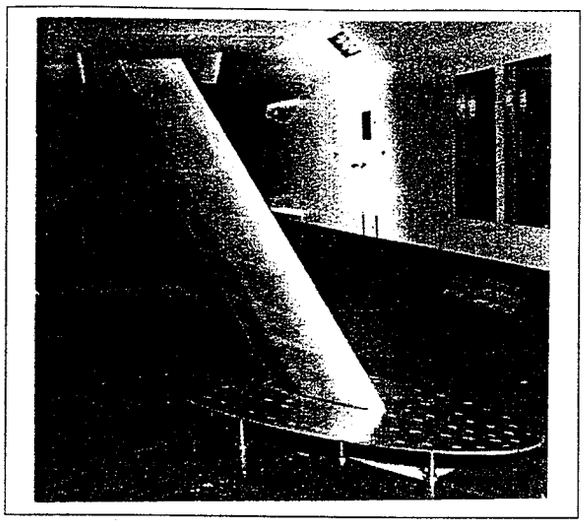

Figure 1: Model 2337 in the 13ft x 9ft wind tunnel.

Experimental results

Experimental details

The 13ft x 9ft tunnel is a closed circuit, continuous operation atmospheric low speed facility. The model is shown in figure 1 mounted on the half model rig to a four component mechanical balance suspended below the turntable. The model is a constant chord wing with no taper or twist, and has been designed with a large amount of rear camber. The wing section (normal to sweep) is derived from the supercritical aerofoil RAE5225 and has a 14% thickness/chord ratio. The leading edge of the datum aerofoil is drooped to ensure attached flow in this region at high incidence. Sufficient trailing-edge droop was also applied to provide a strong adverse pressure gradient, typical of a transonic manoeuvre condition, and ensures that flow breakdown occurs in this region at sweep angles of interest.

A splitter-plate is mounted horizontally above the tunnel floor to avoid interactions between the wing root flow and the relatively thick boundary layer on the working section floor. Force and moment measurements were taken and wing surface pressure measurements at five stations. Flow visualisation studies were made using the oil flow technique. Transition was fixed on both upper and lower surfaces at 5% chord. Corrections to force, pressure and angle of incidence measurements were made to account for instrumentation drifts and the effects of constraint in a solid wall wind tunnel[1, 2].

Two series of tests were performed, providing data at three wing sweeps; Λ = 30°, 40° and 50°, at free stream speeds and angles of incidence in the range 30 to 80 m/s and -6° to +16° respectively, for a Reynolds number based on wing streamwise chord, $R_c = 4.2 \times 10^6$.

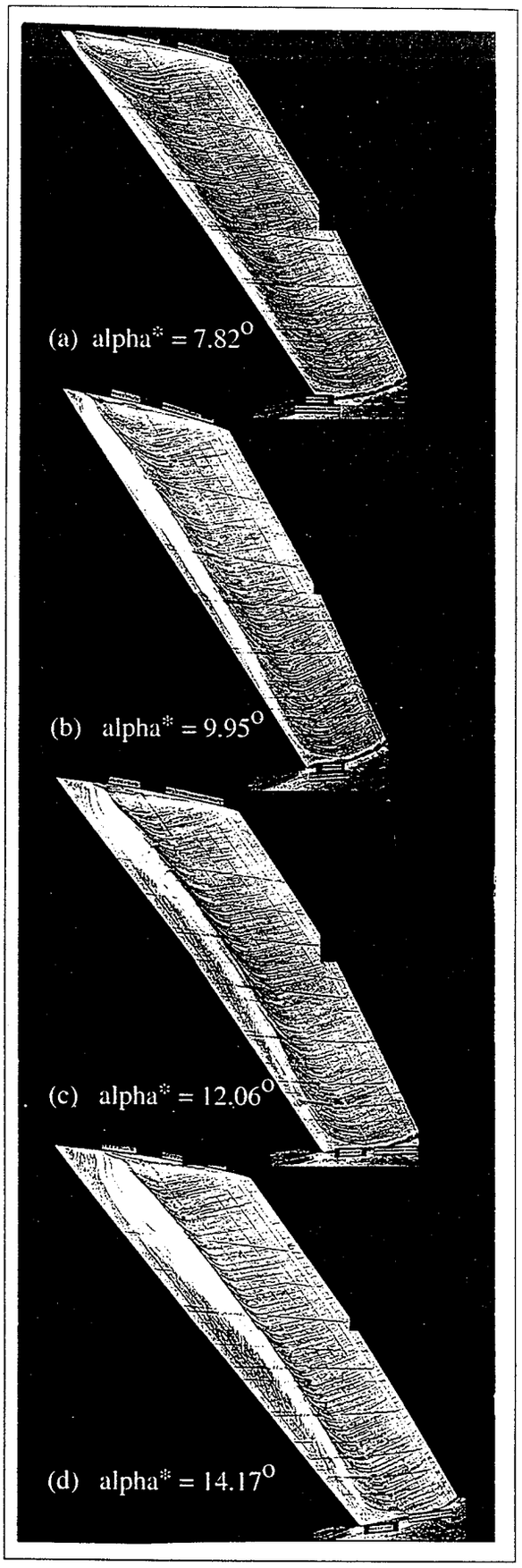

Figure 2: Upper-surface oil flow patterns on basic wing, Λ = 40°, V_∞ = 60m/s.

A discrepancy between measured angle of incidence and that used for CFD calculations exists due to variations in flow angularities and/or setting-up errors positioning the model in the wind tunnel. Hence, comparisons are based on an angle of incidence, α^*, where;

$$\alpha^* = \alpha - \alpha_0$$

and α_0 is the angle of incidence for zero local lift coefficient, derived from integrated pressure distributions at each station on the wing. Although there is variation of $\Delta\alpha_0 = 0.7°$ across the wing span from experimental data ($\Lambda = 40°$, $V_\infty = 60$m/s), a mean value for the five stations is used, giving $\alpha_0 = -5.3°$. Analysis of CFD results gives smaller spanwise variations, and mean values; $\alpha_0 = -6.5°$ from SAUNA data and $\alpha_0 = -6.1°$ from VFP data.

Basic wing flows

Figures 2a to 2d show photographs of oil flow patterns over a range of incidence for a speed of 60m/s and a wing sweep of 40°. Because of the size of the model, it was necessary to take separate photographs of the inboard and outboard wing and match the two, hence the leading edge notch in figure 2. The flows are characterised both by the oil flows and pressure distributions, and they indicate a complex three-dimensional separation, with the separation line moving forward with increasing incidence shown in figure 2. The surface flow direction over the forward part of the wing is almost normal to the leading edge with the angle of the surface streamlines decreasing over the rear section, where the pressure gradients (and therefore crossflows) are most severe, until the streamlines are almost parallel to the trailing edge. Downstream of this position the flow separates into a vortical flow pattern. Although the shear layers are highly three-dimensional due to the large crossflows, the flow is essentially that of an infinite swept wing except near tip and root regions. A vortex is shed from the tip leading edge, which delays the separation position further downstream in this region. The flow development at 50° sweep is similar to that for 40°. In contrast, at the lowest sweep ($\Lambda = 30°$), oil flow patterns indicate that two-dimensional separation is more likely to occur, leading to a closed separation 'bubble'.

Force measurements indicate that for a given lift coefficient, wing drag coefficient increases with wing sweep due to the increasing extent of the separated region leading to an increase in the induced drag component.

Flow control

During the second wind tunnel test, attempts were made to control the flow using cropped-delta vane-type vortex generators that were co-rotating and toed out. The devices produce trailing vorticity which mixes high energy air from the inviscid external flow with low energy flow within the boundary layer. The net effect is to (a) make the boundary layer thinner and hence less likely to separate; and (b) relax the tendency for outward drift in the boundary layer, thus delaying the point of separation. Tests on the wing swept to 40° at a speed, $V_\infty = 60$m/s, and a range of angles of incidence reveal that a suitable configuration of vortex generators would delay separation, almost doubling the lift coefficient for buffet onset (based on an analysis of the variation in measured trailing edge pressure coefficient with lift coefficient). Reductions in lift dependent drag factor of up to 10% for lift coefficients above 0.4 were also measured.

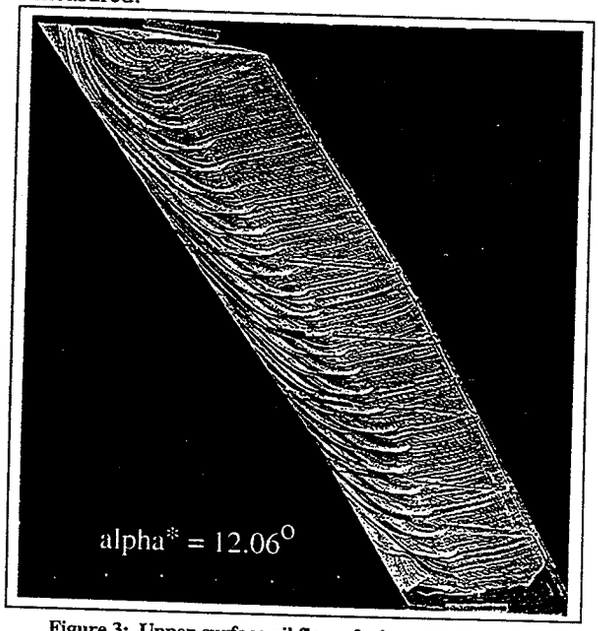

Figure 3: Upper-surface oil flow of wing with flow control, $\Lambda = 40°$, $V_\infty = 60$m/s.

Although most configurations of vortex generators were successful in delaying separation to some extent, it was possible to deduce optimum values of chordwise position, angular deflection, spanwise spacing and vane size/shape for minimum drag. Though a large vane produces greater trailing vorticity and is more effective in controlling separation, it also has higher parasitic drag and is not necessarily optimum. Vane height should be approximately that of the local boundary layer thickness, with an angular deflection to the freestream direction of about 20° and a chordwise position 0.05c upstream of the separation line. The optimum values were found to be similar to those recommended by an ESDU data item[3] for

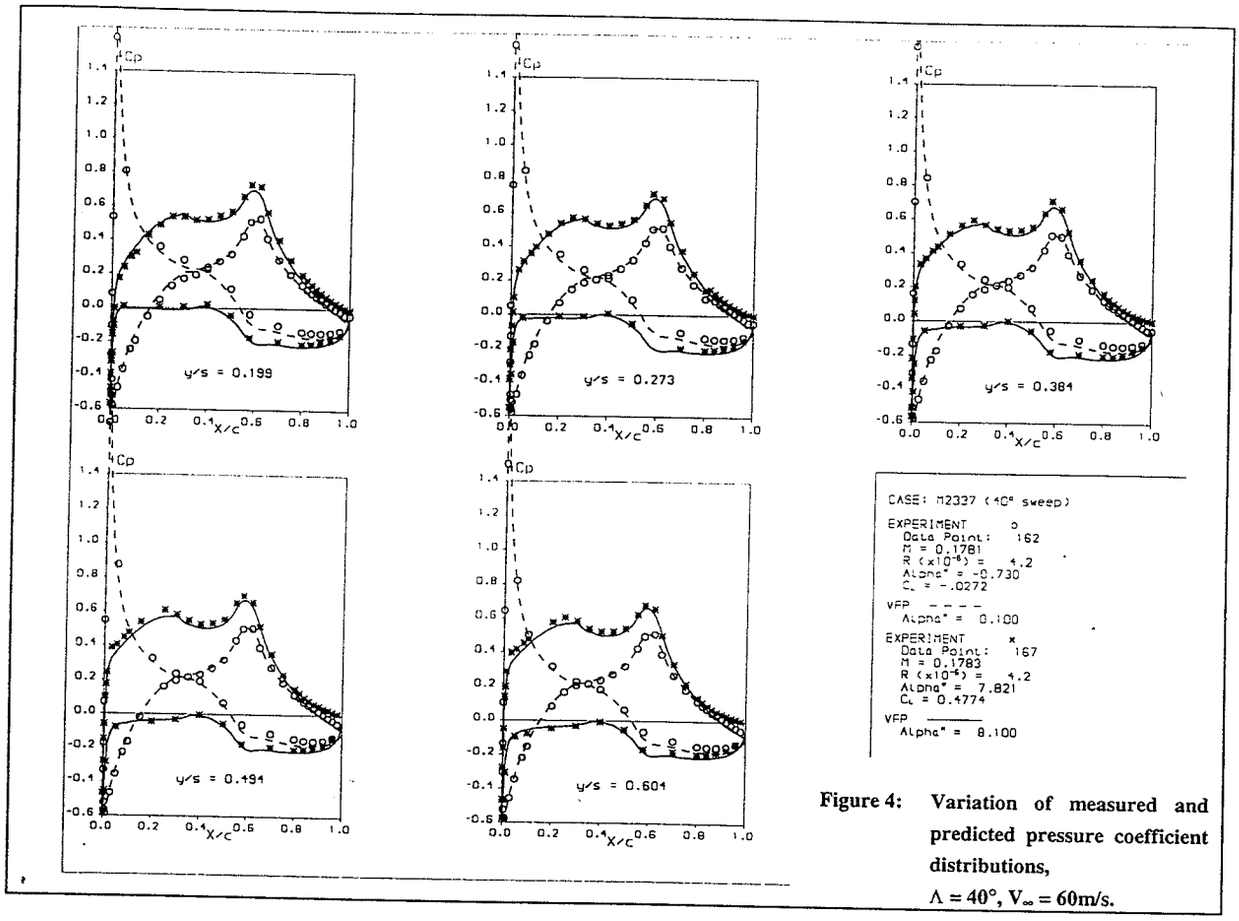

Figure 4: Variation of measured and predicted pressure coefficient distributions, $\Lambda = 40°$, $V_\infty = 60$m/s.

controlling shock induced separation, though ESDU recommend a smaller angular deflection and a position further upstream from the separation line. Figure 3 shows an oil flow on the wing upper surface, indicating how flow control delays separation to the trailing edge for an angle of incidence, $\alpha^* = 12.1°$, compared with the basic wing flow shown in figure 2c. Results from this study are described in more detail in Reference 4.

CFD results

Calculations have been performed using CFD methods ranging in complexity from a viscous coupled full-potential method (VFP) to a Reynolds averaged Navier-Stokes (RANS) solver. 'Free-air' conditions are simulated as opposed to 'in-tunnel' conditions, implying that the flow around the model is similar to that of an equivalent 'free-air' flow. All calculations are performed to convergence levels representing at least a three order reduction in magnitude of the residuals and are concentrated on a wing sweep of 40°. At this sweep, the pressure tappings on the wing are inclined at 5° to the freestream direction, though comparisons with CFD data are assumed along streamwise cuts. An examination of pressure distributions indicates that the variation of pressure coefficient along a generator is sufficiently small for the difference between the two cuts to be ignored.

VFP calculations

The Viscous coupled Full-Potential code (VFP), is based on a viscous-inviscid interaction procedure, combining a numerical solution of the full-potential flow equations for the equivalent inviscid flow with a swept and tapered semi-inverse procedure for calculating shear layers. Figure 4 compares experimental pressure distributions with those predicted using VFP at angles of incidence, $\alpha^* = 0.1°$ and $8.1°$, for $\Lambda = 40°$, $V_\infty = 60$m/s, and a Reynolds number (based on wing streamwise chord) of 4.2×10^6. Both sets of results show pressure distributions with close agreement and strong adverse pressure gradients over the rear of the sections. However, VFP predicts a higher pressure at the trailing edge, and therefore, a better pressure recovery than was measured indicating an inability to model the separated flow in this region. A converged solution could not be attained for higher angles of incidence.

SAUNA method

Reynolds-averaged Navier-Stokes methods have therefore been used to assess the ability to predict

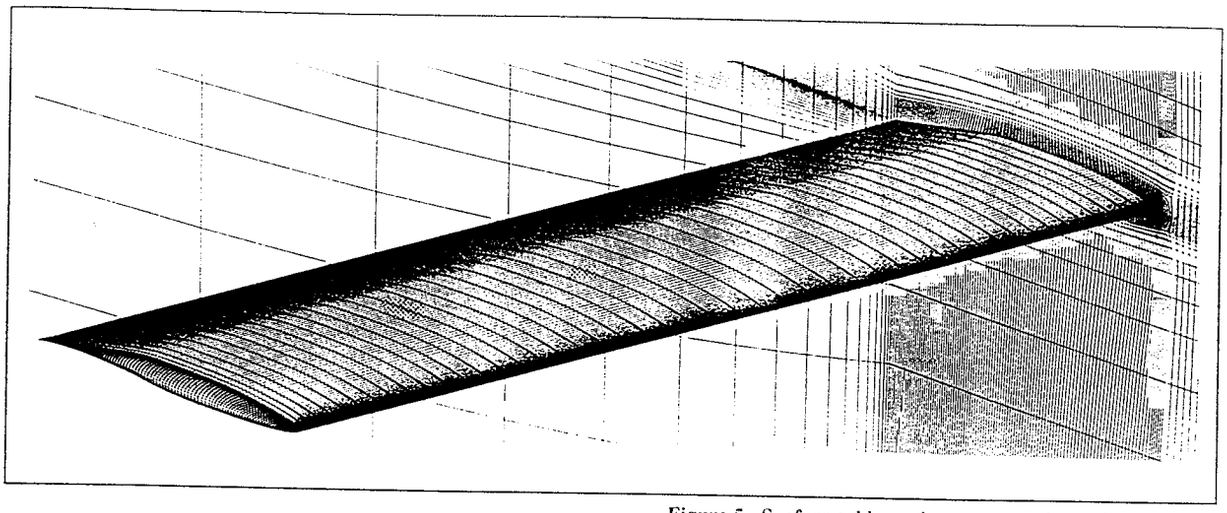

Figure 5: Surface grids on the wing and plane of symmetry

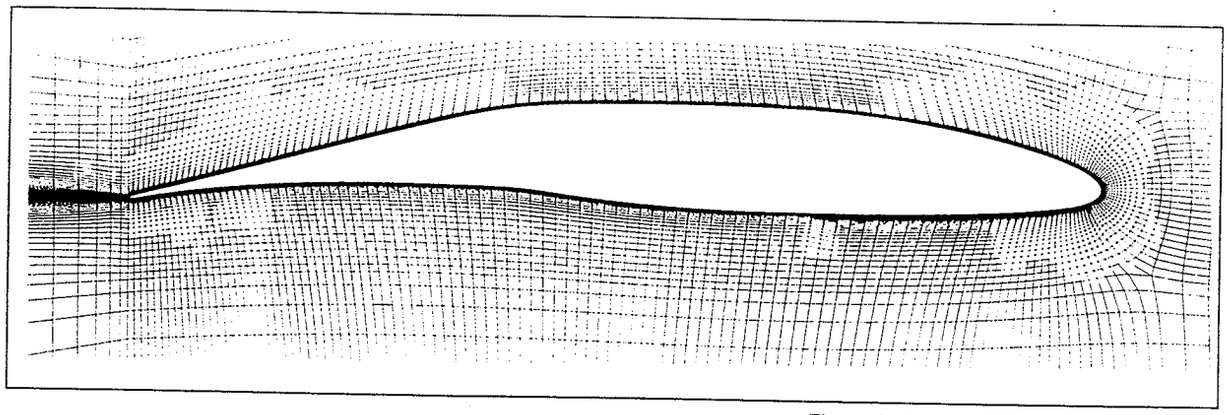

Figure 6: Cut through the refined field grid

these complex flows. In particular, calculations have been made using the SAUNA[5] (Structured And Unstructured Numerical Analysis) system. A structured multiblock grid has been generated for the wing at a sweep of 40° with refinement near the wing surface suitable for a solution of the Navier-Stokes equations. To simulate these complex flows, with highly curved boundary layer streamlines and strong adverse pressure gradients, a two-equation k-ω turbulence model is recommended[6] and is employed for these calculations. A multigrid convergence acceleration technique is also used.

Initial calculations revealed pressure coefficient oscillations on the wing surface due to discontinuities in surface curvature, where camber had been applied to the datum RAE5225 aerofoil. Refinement of the grid in this region reduced these oscillations without the need for geometry smoothing. A topology of 120 blocks was formed, with 'C' topologies embedded around the leading edge and tip of the wing. Several control planes were included within the domain, which can be edited to aid grid control. The grid generated has 233 points defining the wing section, a total of 532,608 cells in the Euler grid and 981,504 cells in the refined Navier-Stokes grid. The grid on the wing upper surface (figure 5) shows grid points clustered near the leading and trailing edge of the wing and at the tip and root where solution activity is greatest. The figure indicates that the wing tip geometry has been rounded to improve the quality of the field grid that wraps around the wing tip. Though the wind tunnel model has a straight tip, it is not thought that this feature will have a significant effect on the overall flow development. Further grid refinement has little impact on wing surface pressure distributions.

For the k-ω turbulence model an initial grid spacing normal to the wing surface of $Y+ < 1$ is required for the correct prediction of shear layers where,

$$Y^+ \approx D.R_c.\sqrt{\frac{C_f}{2}}$$

and D is the actual dimension of the first grid point from the wing surface and C_f is determined for a flat plate at the required flow conditions. A section through the finest level of the refined grid is shown in figure 6 and indicates good orthogonality.

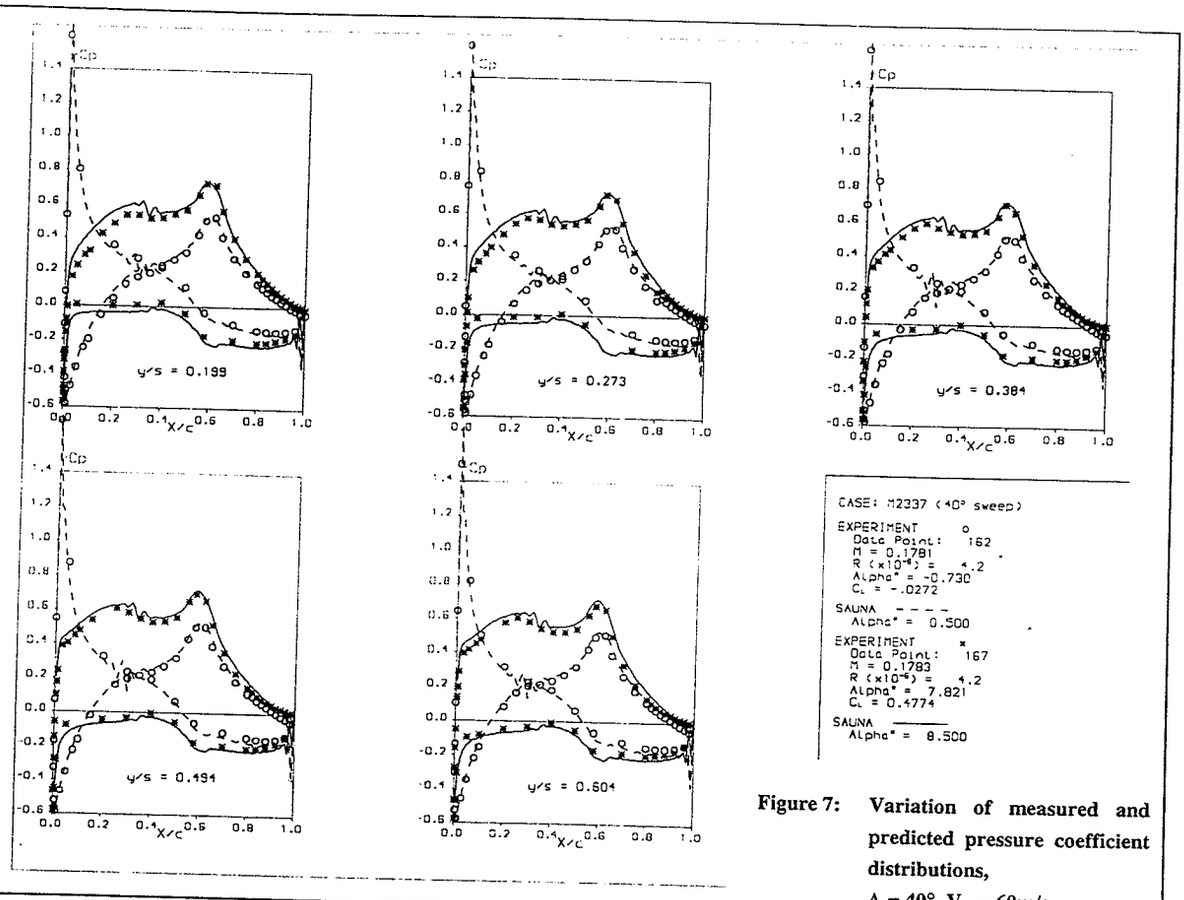

Figure 7: **Variation of measured and predicted pressure coefficient distributions, $\Lambda = 40°$, $V_\infty = 60$m/s.**

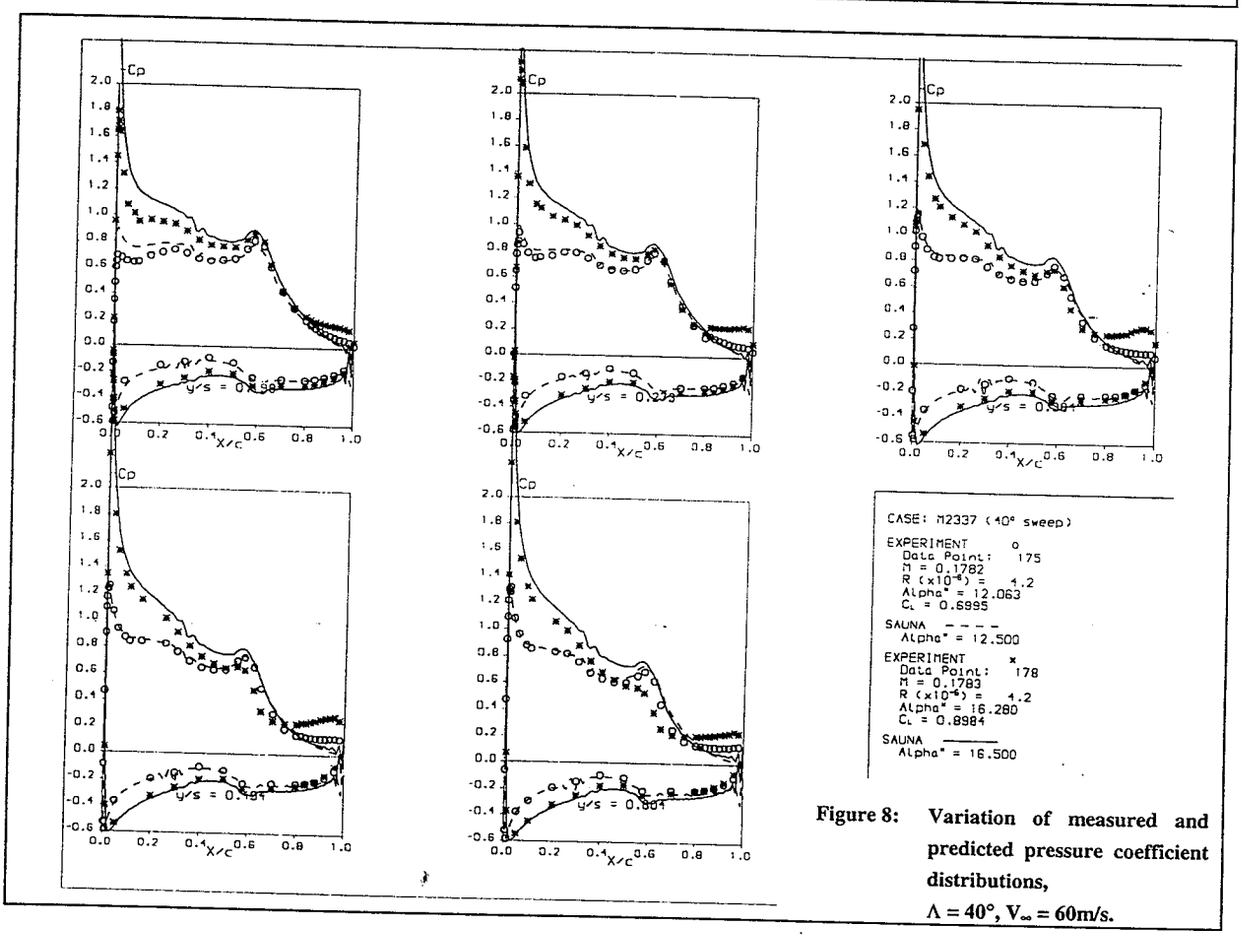

Figure 8: **Variation of measured and predicted pressure coefficient distributions, $\Lambda = 40°$, $V_\infty = 60$m/s.**

Although an attempt was made to model the viscous flow over the splitter plate used in the experiment, only small improvements in wing surface pressure distribution on the inboard wing were achieved. Consequently, end plate modelling in further calculations has been neglected since only a small region of the flow is affected, whilst refinement of the end plate grid contributes a significant increase in grid size and, therefore, computer resources.

SAUNA results

Calculations were performed on this grid for a compressible flow with a freestream Mach number of 0.178 (V_∞ = 60m/s), $R_c = 4.2 \times 10^6$ and angles of incidence, $\alpha^* = 0.5°$, 8.5°, 12.5° and 16.5°. Figures 7 and 8 compare the experimental and predicted pressure distributions. In general, the angles of incidence are greater than experimental values shown in figures 7 and 8, giving a higher wing loading than experimental results due to greater suction levels on the upper surface near the leading edge. Although the adverse pressure gradients match reasonably well, figure 8 shows that flow breakdown is not predicted. For angles of incidence, $\alpha^* = 12.06°$ and 16.28°, experimental pressure distributions show a plateau in pressure coefficient corresponding to the separated flow region, which SAUNA does not predict. A further calculation using a more advanced Multiscale Reynolds Stress model (without wall functions), did not improve the modelling of the trailing edge flow at $\alpha^* = 8.5°$.

Discussion and Conclusions

A combined experimental and theoretical study of the low speed flow over a variable sweep model, for trailing edge sweeps greater than 30° has been described.

This study has indicated that high wing sweep has an important impact on the manoeuvre performance of an aircraft. The highly cambered wing section used for this investigation generates strong adverse pressure gradients over the rear of the section leading to complex three-dimensional separations. Flow visualisation and pressure measurements on the wing surface have indicated the mechanism for the flow breakdown, whilst providing information which allow flow control devices to be successfully positioned. It has been shown that this complex flow can be controlled using a suitable configuration of vane-type vortex generators, giving significant performance benefits.

There is a need to be able to compute these flows at flight conditions, particularly to locate and characterise regions of separated flow so that control devices can be incorporated early in the design cycle, rather than as 'add-ons' to solve problems encountered during flight test. This could also allow control devices to be used to provide novel solutions to multidisciplinary wing design problems.

Calculations using the Viscous coupled Full Potential CFD code have given good agreement with experiment for a wing sweep of 40°, except near the trailing edge region. Reynolds averaged Navier-Stokes calculations using the SAUNA CFD system have given reasonable agreement with experimental pressure distributions but do not predict flow separation. However, initial Reynolds averaged Navier-Stokes solutions (described in reference 7) on a coarser grid, relative to that used for the present study, predicted regions of separated flow in the trailing edge region which were in good comparison with experimental results. The geometry for these calculations was smoothed, resulting in poor representation of the leading edge flow development. In comparison, the present grid has Y+ values at the wing surface which are an order of magnitude smaller and has significantly more cells in the grid. Although leading edge flows presented here are well represented, the present grid may be less suitable for predicting the flow at high angle of incidence, where grid definition in the region of the separated shear layers is inadequate. Because initial grid spacing has been based on the flat plate representation of skin friction coefficient, initial spacings on the rear of the upper surface, where skin friction is very small or negative, are not suitable for this type of flow. Indeed, the coarser grid described in reference 7 may have provided better grid resolution for separated shear layers. Further CFD investigations are required to build confidence in the methods ability to model such complex flows. Indeed, the complex flow field around this relatively simple geometry provides a difficult test case for CFD methods to predict.

CFD calculations are not sufficiently mature at present to be able to predict this flow with confidence, highlighting the necessity to continue experimental studies in order to demonstrate wing performance.

References

1. "Subsonic wind tunnel wall corrections." H C Garner, W E Rogers, W E A Acum and E C Maskell, AGARDograph 109, October 1966.

2. "Corrections for symmetric swept and tapered wings in rectangular wind tunnels." W E A Acum, R&M 2777, April 1950.
3. "Vortex generators for control of shock-induced separation." ESDU data item on Transonic Aerodynamics, Volume 5, November 1996.
4. "Effectiveness of vortex generator positions and orientations on highly swept wings." J I Broadley and K P Garry, AIAA 97-2319, June 1997.
5. "Validation and evaluation of the advanced aeronautical CFD system SAUNA - a method developer's view." J A Shaw, J M Georgala, P N Childs, C A McHugh, N E May and A J Peace, Paper 3, 1993 European Forum on Recent Developments and Applications in Aeronautical CFD, September 1993.
6. "Turbulence Modeling for CFD." D C Wilcox, DCW Industries, Inc., 1993.
7. "Trailing-edge flows on highly-swept wings." A Shires, AIAA 97-2205, June 1997.